

Original Research

Research on Displacement Diffusion Model of Time-Varying Slurry with Rheological Parameters in Unsaturated Media

Zhanlin Mu¹, Fengxi Zhou^{1, 2*}

¹School of Civil Engineering, Lanzhou University of Technology, Lanzhou, Gansu 730050, China

²Engineering Research Center of Disaster Mitigation in Civil Engineering of Ministry of Education, Lanzhou, Gansu 730050, China

Received: 15 March 2023

Accepted: 25 April 2023

Abstract

The estimation of grouting pressure and slurry diffusion range in grouting engineering is an urgent engineering problem to be solved, as the diffusion behavior of slurry is extremely concealed and the geological structure of underground rock and soil is complex. Taking power-law slurry as the research object, the seepage movement equation of time-varying slurry is obtained by analyzing the laminar flow movement of the slurry in the circular pipe. A cylindrical diffusion model considered the displacement of slurry-water-gas is established based on the theory of seepage in unsaturated porous media. Combined with the seepage motion equation, relevant boundary conditions and interface conditions, the power-law slurry diffusion equation is obtained, which takes into account the principal grouting parameters and mechanical parameters. At the same time, the rheological characteristics and viscosity time-varying experiment of slurry are carried out to obtain the rheological and consistency coefficient time-varying curves of slurries with different water-cement ratio, as well as corresponding function expressions. Then the numerical examples are used to analyze the mechanism of different factors affecting the slurry diffusion behavior. The above analysis and experimental results confirm the effectiveness and applicability of the research results, which can provide necessary theoretical support and technical reference for the design and construction of grouting projects in unsaturated soil areas.

Keywords: displacement effect, rheological parameters time-varying, power-law slurry, cylindrical diffusion, unsaturated media

Introduction

With the rapid pace of infrastructure construction in China, the geological conditions faced in projects such as buildings, roads, mines and water conservancy have become increasingly complex, leading to a series of engineering quality problems. Grouting technology has been widely used as an effective means to solve various engineering quality problems [1-3]. However, the current research on the grouting mechanism and the evaluation of the grouting effect lags far behind the engineering practice, among which how to predict the grouting pressure, control the slurry diffusion radius and thus improve the grouting efficiency are urgent problems in theoretical research.

Common grouting materials, such as cement slurry, are not a single flow pattern, and can be divided into power-law fluid, Bingham fluid and Newtonian fluid according to the rheological constitutive equation [4]. Most of the current studies on slurry diffusion laws are based on Newtonian slurry [5-7] and Bingham slurry [8-10], with little in-depth research on power-law slurry. Among them, Mu et al. [11] took the power-law slurry with low water-cement ratio commonly used in engineering as the research object, established a slurry flow model in rough cracks and provided a calculation method for grouting parameters of cement-based slurry, while using experiments to verify the effectiveness of the above method. Zou et al. [12] extended the two-phase flow model of Bingham fluid in a single fracture, and investigated the propagation of power-law slurry in random fracture network based on the above extended model. Subsequently, he proposed the analytical solution of unidirectional radial flow including yield-power-law fluid, and combined it with the radial flow model of two-phase flow in homogeneous fractures to explain the relationship between the pressure distribution and the slurry diffusion radius during grouting [13]. Based on the Hele-Shaw smooth plate model, Zhang et al. [14] derived the relationship between slurry diffusion radius and grouting time when the power-law slurry diffuses in the single fracture plate model by using the force balance equation of fluid micro-unit, the rheological equation and the mass conservation equation of power-law fluid in the column coordinate system.

A large number of engineering practices show that the rheological properties of slurry will be significantly affected by time changes, and directly affect the diffusion state of slurry [15-16]. Based on this feature, many scholars combined the viscosity time-varying function expression with the seepage movement equation to obtain the slurry diffusion equation under different working conditions when deriving the theoretical formula [17]. At the same time, the influence of the time-varying characteristics of slurry viscosity on the grouting effect is analyzed. Through calculation comparison and experimental verification,

it is shown that fully considering the variation rule of slurry viscosity with time will greatly improve the applicability and accuracy of the grouting theory [18], which is a further improvement of the power-law grouting theory. However, the properties and flow patterns of cement slurry differ significantly from those of water [19], so the traditional slurry diffusion model proposed based on a single-flow model that takes groundwater into account as a definitive boundary is not accurate. The two-phase flow process of slurry and water is essentially slurry-water displacement. Ye et al [20] considered the displacement effect of power-law slurry on groundwater and simplified the seepage movement equation of power-law slurry to obtain the slurry diffusion equations under the cylindrical and spherical diffusion forms respectively. It can be seen that the characteristics of unsaturated medium are either ignored in the study of slurry diffusion mechanism, or the existing unreasonable theoretical system of saturated soil mechanics is directly applied to simplify the solution. In recent years, Yang et al. [21] combined the relevant theories of unsaturated soil with the permeability potential function model to investigate the mechanism of slurry diffusion when grouting behind the shield tunnel wall in unsaturated strata, and obtained the calculation formulae of slurry diffusion radius under three different unsaturated strata conditions. In grouting engineering practice, the influence of soil saturation (water content) on grouting effect cannot be ignored. By carrying out a series of indoor pressure grouting tests, direct shear tests and microscopic observation and analyzing the test results, it can be known that different soil saturation will lead to different grouting characteristics, thus making the final engineering efficiency completely different [22].

Based on this, this paper takes the time-varying power-law slurry as the research object, and considers the displacement effect of slurry in the diffusion process of unsaturated injected medium. Using the seepage theory of unsaturated porous media, a time-varying power-law slurry diffusion equation is established, which comprehensively considers many factors, such as water-cement ratio, injected media saturation, grouting pipe radius, grouting time, soil inherent permeability and porosity. At the same time, the rheological characteristics and viscosity time-varying experiment of cement slurry are carried out, and the theoretical results are degraded to the saturated state, and combined with the experimental results to compare and verify with the existing research results. Finally, numerical examples are used to analyze the specific mechanism of different influencing factors to verify the validity and accuracy of the research results in this paper, so as to provide necessary theoretical support and technical reference for the construction and design of water control and seepage prevention of mine roadway and reinforcement of tunnel surrounding rock and karst strata in unsaturated soil areas.

Theory

Cylindrical Diffusion Model

The slurry cylindrical diffusion model is shown in Figure 1. During the grouting process, the slurry is driven by the grouting pressure and enters the surrounding injected medium in the form of cylindrical diffusion through the grouting holes on both sides of the grouting pipe, thus completing the subsequent process of slurry migration diffusion and reinforcement. In Fig. 1, p_0 is the grouting pressure, r_0 is the radius of grouting pipe, m is the height of slurry column, p_g is the slurry pressure, p_k is the pore fluid pressure, and R is the radius of interface between slurry and pore fluid after time t .

For unsaturated soils, considering the connectivity of the aeration pores of the soil, where the pore gases within the soil are connected to the outside atmosphere. so the pore gas pressure relative to the atmospheric pressure is 0, that is, $p_a = 0$, the initial conditions are as follows:

Initial conditions at moment $t = 0$:

$$\varphi(0) = r_0, S_r = S_r^0 \tag{1}$$

Where S_r and S_r^0 are the degree of saturation of soil and its initial degree of saturation respectively.

At $t > 0$, the position of the interface between slurry and pore fluid is $\varphi(t) = R$, and the corresponding boundary conditions are given as follows:

$$p_g|_{\varphi=r_0} = p_0 \tag{2}$$

$$p_g|_{\varphi=R} = p_{cr} \tag{3}$$

$$(S_r p_w)|_{\varphi=R} = p_{cr} \tag{4}$$

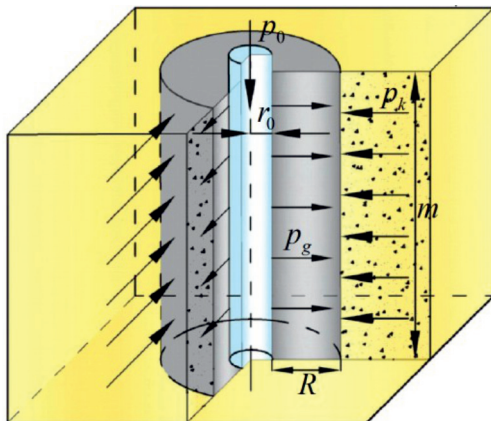


Fig.1. Cylindrical diffusion model of slurry.

$$p_w|_{\varphi=r_e} = p_w^0 \tag{5}$$

Where p_{cr} is the pressure at the interface between slurry and pore fluid, p_w is the pore water pressure, r_e is the farthest disturbance range to pore fluid during slurry diffuses, and p_w^0 is the initial pore water pressure.

At $t > 0$, the seepage continuity conditions of slurry and pore fluid is as follows:

$$\varphi(t) = R, v_g = S_r v_w \tag{6}$$

Where v_g is the slurry seepage rate, and v_w is the pore fluid seepage rate.

Infiltration Diffusion Analysis

Basic Assumptions

In this paper, the following assumptions are made when studying the diffusion law of time-varying power-law slurry under displacement effect [23, 24]:

1. The injected unsaturated soil medium is homogeneous and isotropic elastic-plastic material.
2. In the process of diffusion and displacement of power-law slurry in unsaturated porous media, its flow velocity is small and its flow regime remains laminar all the time.
3. The power-law slurry is incompressible and its rheological index does not change with time during grouting, that is $n_0 = n(t)$.
4. The self-weight effect of the grout is ignored during grouting.

Seepage Motion Equation

The rheological equation of power-law slurry is as follows:

$$\tau = C \gamma^n \tag{7}$$

Where τ is the shear stress, C is the consistency coefficient, $\gamma = -\frac{dv}{dr}$ is the fluid shear rate, and n is the rheological index.

During the injection process, the consistency coefficient of the power-law slurry has obvious time-varying characteristic, and its time-varying function is expressed as:

$$C(t) = C_0 e^{\beta t} \tag{8}$$

Where C_0 is the initial consistency coefficient of power-law slurry, and β is the time-varying coefficient of consistency.

Combining Equations (7) and (8), the rheological equation of time-varying power-law slurry can be obtained as follows:

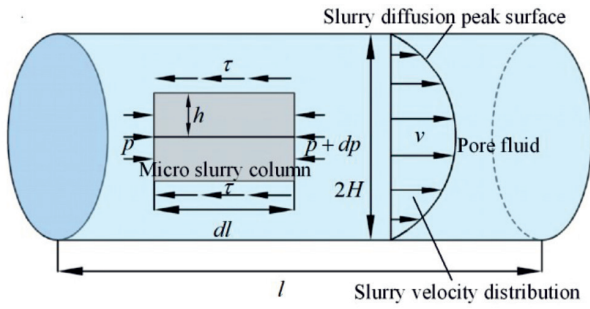


Fig. 2. Schematic diagram of Micro-element slurry column flow in circular pipe.

$$\tau = C_0 e^{\beta t} \gamma^n \tag{9}$$

In order to study the seepage movement equation of time-varying power-law slurry with rheological parameters. As shown in Fig. 2, the laminar motion of power-law slurry in a circular tube with radius H is analyzed.

Taking the micro slurry column in the tube as the research object, its mechanical equilibrium equation is as follows:

$$p\pi h^2 = (p + dp)\pi h^2 + 2\pi h dl \tau \tag{10}$$

Where h is the radius of micro slurry column, and $h < H$, dp is the pressure difference at both ends of the micro slurry column, and dl is the length of the micro slurry column.

Then from Equation (10), the following equation is derived:

$$\tau = -\frac{h}{2} \frac{dp}{dl} \tag{11}$$

Substituting Equation (11) into Equation (9) produce the shear rate of the power-law slurry:

$$\gamma = -\frac{dv}{dh} = \left(-\frac{1}{2C_0} \frac{dp}{dl} \right)^{1/n} h^{1/n} \tag{12}$$

By integrating Equation (12) and combining the boundary condition $h = H, v = 0$. at the pipe wall, the equation of velocity of power law slurry in a circular tube with radius H can be obtained as follows:

$$v = \left[\left(-\frac{1}{2C} \frac{dp}{dl} \right)^{1/n} \frac{n}{1+n} \right] \left(H^{\frac{1+n}{n}} - h^{\frac{1+n}{n}} \right) \tag{13}$$

Therefore, the flow rate Q_p of power-law slurry flows in a circular pipe with radius H is as follows:

$$Q_p = \pi \left(-\frac{1}{2C_0 e^{\beta t}} \frac{dp}{dl} \right)^{1/n} \frac{n}{1+3n} H^{\frac{1+3n}{n}} \tag{14}$$

According to Equation (14), the average flow velocity at the cross-section of the circular tube is as follows:

$$\bar{v} = \frac{Q_p}{\pi H^2} = \left(-\frac{1}{2C_0 e^{\beta t}} \frac{dp}{dl} \right)^{1/n} \frac{n}{1+3n} H^{\frac{1+n}{n}} \tag{15}$$

Combining with the D-F relational formula, that is, $v_g = \phi \bar{v}$, and the seepage motion equation of power-law slurry can be expressed as:

$$v = \phi \bar{v} = \phi \left(-\frac{1}{2C_0 e^{\beta t}} \frac{dp}{dl} \right)^{1/n} \frac{n}{1+3n} H^{\frac{1+n}{n}} \tag{16}$$

The effective viscosity μ_e and effective permeability K_e of the power-law slurry are introduced and expressed as:

$$\begin{cases} \mu_e = C_0 e^{\beta t} \left(\frac{1+3n}{\phi H n} \right)^{n-1} \\ K_e = \frac{\phi H^2}{2} \left(\frac{n}{1+3n} \right) \end{cases} \tag{17}$$

Combining with the inherent permeability of the injected medium $K = \frac{\phi H^2}{8}$, it can be obtained as:

$$\begin{cases} \mu_e = C_0 e^{\beta t} \left(\frac{1+3n}{n} \right)^{n-1} (8\phi K)^{\frac{1-n}{2}} \\ K_e = 4K \left(\frac{n}{1+3n} \right) \end{cases} \tag{18}$$

Combining Equations (16) and (17), the seepage velocity of power-law slurry is derived:

$$v_g = \left(\frac{K_e}{\mu_e} \right)^{1/n} \left(-\frac{dp}{dl} \right)^{1/n} \tag{19}$$

Analysis of Displacement Effects

When pressure grouting is carried out in unsaturated water-bearing strata, the subsequent diffusion reinforcement process of the slurry injected into the surrounding soil through the grouting pipe cannot be defined simply as the seepage process of a single-phase fluid in porous media. In fact, the slurry is driven by the grouting pressure to drive and squeeze the pore fluid in the unsaturated porous medium, which is the driving process. The slurry then occupies the position of the original pore fluid and takes its place, which is the replacement process. The whole process described above is a complete process of multiphase fluid seepage displacement in unsaturated porous media.

Displacement Model

The application of displacement model in the field of oil and gas development has been relatively mature, such as oil and gas production technology of water pressure drive oil. Different from the obvious interface between oil and gas two immiscible fluids in petroleum exploitation engineering [25-27]. When the slurry in the water-bearing stratum of unsaturated soil is displacing and diffusing, there is a certain miscibility between slurry and pore fluid, so a thin miscible transition zone is formed. However, the range of the miscible transition zone is smaller than the final diffusion radius of the slurry. For the convenience of calculation, the miscible transition zone is simplified as a mutation interface that is, one side is the slurry flow zone and one side is the pore fluid zone. And the pressure and flow at the interface are continuous.

As shown in Fig. 3, the position of the mutation interface between the cement slurry and the pore fluid changes over the grouting time as it permeates and diffuses under continuous grouting pressure. That is,

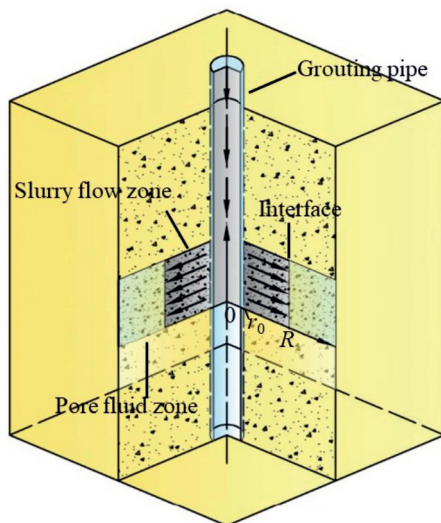


Fig. 3. Schematic diagram of slurry seepage under displacement effect.

there is a certain time t , the distance from the interface to the origin $x = 0$ is φ , and the interface equation can be obtained as follows:

$$F(x, t) = x - \varphi(t) = 0 \tag{20}$$

And

$$\varphi(0) = r_0 \tag{21}$$

$$\varphi(t) = R \tag{22}$$

When the power-law slurry is taken as the research object for analysis and derivation, it satisfies the generalized Darcy's law. However, the single-phase power-law slurry is different from two-phase pore fluid. It is the inherent permeability K of the injected medium that affects the infiltration and diffusion behavior of the slurry, which is independent of the slurry characteristics of single-phase power-law fluid. Applying the generalized Darcy's law to power-law slurry in the slurry flow zone, the following equation is derived:

$$q_g = -2\pi\varphi m \left(\frac{K_e}{\mu_e} \right)^{1/n} \left(\frac{dp_g}{d\varphi} \right)^{1/n} \tag{23}$$

Where q_g is the flow rate of slurry flow zone.

Differentiating Equation (23), the following equation can be obtained:

$$\frac{d}{d\varphi} \left[\varphi \left(\frac{dp_g}{d\varphi} \right)^{1/n} \right] = 0 \tag{24}$$

Solving the differential Equation (24) gives:

$$p_g = \frac{C_1}{1-n} \varphi^{1-n} + C_2 \tag{25}$$

In the zone of slurry flow area, combining Equations (2) and (3) of boundary and interface conditions and Equations (25), the coefficients C_1 and C_2 can be obtained as follows:

$$\begin{cases} C_1 = \frac{(p_{cr} - p_0)(1-n)}{R^{1-n} - r_0^{1-n}} \\ C_2 = \frac{p_0 R^{1-n} - p_{cr} r_0^{1-n}}{R^{1-n} - r_0^{1-n}} \end{cases} \tag{26}$$

Substituting Equation (26) into Equation (25), the power-law slurry infiltration diffusion equation is given as follows:

$$p_g = \frac{(p_{cr} - p_0)}{R^{1-n} - r_0^{1-n}} \phi^{1-n} + \frac{p_0 R^{1-n} - p_{cr} r_0^{1-n}}{R^{1-n} - r_0^{1-n}} \quad (27)$$

The generalized Darcy's law is also applied to the pore fluid zone, and the following equation is derived:

$$q_w = -2\pi\phi m S_r k_w \frac{dp_w}{d\phi} \quad (28)$$

Where q_w is the flow rate of pore fluid, k_w is the permeability coefficient of pore fluid, and k_w can be expressed as

$$k_w = \frac{K k_{rw}}{\mu_w} \quad (29)$$

Where k_{rw} is the relative permeability of liquid phase, which is related to the degree of saturation, and μ_w is the dynamic viscosity coefficient.

Differentiating equation (28), the following equation can be obtained:

$$\frac{d}{d\phi} \left(\phi \frac{dp_w}{d\phi} \right) = 0 \quad (30)$$

Solving the differential Equation (30) gives:

$$p_w = C_3 \ln \phi + C_4 \quad (31)$$

In the zone of pore fluid, combining Equations (4) and (5) of boundary and interface conditions and Equations (31), the coefficients C_3 and C_4 can be obtained as follows:

$$\begin{cases} C_3 = \frac{p_{cr} - S_r p_w^0}{S_r (\ln R - \ln r_e)} \\ C_4 = \frac{\ln R S_r p_w^0 - p_{cr} \ln r_e}{S_r (\ln R - \ln r_e)} \end{cases} \quad (32)$$

Substituting Equation (32) into Equation (31) produces the pressure distribution in the pore fluid zone:

$$p_w = \frac{p_{cr} - S_r p_w^0}{S_r (\ln R - \ln r_e)} \ln \phi + \frac{S_r p_w^0 \ln R - p_{cr} \ln r_e}{S_r (\ln R - \ln r_e)} \quad (33)$$

Combining Equations (27) and (33) and bringing into Equation (6) of seepage continuity condition gives

$$\left(\frac{K_e}{\mu_e} \right)^{1/n} \left[-\frac{(p_{cr} - p_0)(1-n)}{R^{1-n} - r_0^{1-n}} \right]^{1/n} = S_r k_w \left(-\frac{p_{cr} - S_r p_w^0}{S_r (\ln R - \ln r_e)} \right) \quad (34)$$

During pressure grouting, the total amount of grouting Q of power-law slurry can be expressed as follows:

$$Q' = q_g t = 2\pi m \left(\frac{K_e}{\mu_e} \right)^{1/n} \left[-\frac{(p_{cr} - p_0)(1-n)}{R^{1-n} - r_0^{1-n}} \right]^{1/n} t \quad (35)$$

Where t is grouting time.

The total amount of grouting can also be expressed as

$$Q' = \pi R^2 m \phi \quad (36)$$

Coupling Equations (35) and (36) results in the following equation:

$$\left(\frac{K_e}{\mu_e} \right)^{1/n} \left[-\frac{(p_{cr} - p_0)(1-n)}{R^{1-n} - r_0^{1-n}} \right]^{1/n} = \frac{\phi R^2}{2t} = k_w \left(-\frac{p_{cr} - S_r p_w^0}{\ln R - \ln r_e} \right) \quad (37)$$

According to Equation (37), the pressure p_{cr} at the interface between slurry and pore fluid is given as follows:

$$p_{cr} = S_r p_w^0 - \frac{\phi R^2 \ln R / r_e}{2k_w t} \quad (38)$$

Solving the Equation (37) gives:

$$p_0 = p_{cr} + \frac{\left(\frac{\phi R^2}{2t} \right)^n \mu_e (R^{1-n} - r_0^{1-n})}{K_e (1-n)} \quad (39)$$

Substituting Equation (38) into Equation (39) derives the slurry diffusion equation:

$$p_0 = S_r p_w^0 - \frac{\phi R^2 \ln R / r_e}{2k_w t} + \frac{\left(\frac{\phi R^2}{2t} \right)^n \mu_e (R^{1-n} - r_0^{1-n})}{K_e (1-n)} \quad (40)$$

Equation (40) is a closed-form expression based on multiphase flow model, which fully considers the slurry-water-gas displacement effect and the influence of the time-varying of the power-law slurry consistency coefficient on the slurry diffusion behavior.

It can accurately describe the relationship between the grouting pressure and many grouting parameters, as well as physical and mechanical parameters when power-law slurry infiltrates and diffuses in unsaturated soil.

It should be noted that the cylindrical infiltration diffusion model of power-law slurry proposed in this paper is based on the laminar flow state of power-law slurry. The flow pattern of power-law slurry in diffusion, namely laminar flow or turbulent flow, can be determined according to its stability coefficient Z [28]. The stability coefficient Z is based on the laminar flow stability theory, that is, when the flow state of the fluid changes from laminar flow state to turbulent flow state, the vortex of turbulence will first appear in the layer with the largest turbulence in the liquid flow, not in the whole pipe diameter section at the same time. The stability coefficient Z is also related to many parameters such as rheological index n , consistency coefficient C , average fluid velocity \bar{v} , tube diameter d (in this paper, it refers to the pore channel diameter of porous media) and slurry density ρ . It can be calculated using the following equation:

$$Z = \frac{n}{2^n} \left(\frac{1}{n+2} \right)^{\frac{n+2}{n+1}} \left(\frac{3n+1}{n} \right)^{2-n} \frac{\bar{v}^{2-n} d^n \rho}{C} \quad (41)$$

When the slurry flow pattern is Newtonian fluid or Bingham fluid, its rheological index $n = 1$ and $Z = 3849R_e$. $R_e = 2100$ is the lower critical Reynolds number for judging laminar and turbulent flow. Therefore, $Z = 808$ can be used to determine the flow state of power-law slurry when it is infiltrating and diffusing in unsaturated porous media, that is, when $Z < 808$, the flow state of power-law slurry is laminar flow; When $Z > 808$, the flow state of power-law slurry is turbulent flow.

Experimental

In order to deeply research the rheological properties and viscosity time-varying characteristics of power-law slurry, the rheological experimental research of slurry is carried out to master the rheological parameters of power-law slurry with different water-cement ratios and draw its rheological curve, so as to fit the rheological equations of slurry with different water-cement ratios. Then, by analyzing the viscosity changes in different time periods, the time-varying equation and curve of the consistency coefficient are obtained by fitting.

The grouting material is ordinary Portland cement of P·O42.5 produced by Qilian mountain cement plant in Yongdeng County, Gansu Province. It has good frost resistance, impermeability and wear resistance, and is widely used in grouting engineering practice, meeting the application requirements. Its specific surface area is 334 m²/kg, and its particle size characteristics are shown

Table 1: Particle size characteristics of cement.

Particle size range	Interval distribution /%
≤5 μm	10.38
5~35 μm	73.74
≤35 μm	84.12
35~65 μm	15.52
≤65 μm	99.64

in Table 1. And the content of various components and material characteristics is shown in Table 2. The experimental equipment is six-speed rotary viscometer of ZNN-D6B type, as shown in Fig. 4. This instrument is a typical coaxial cylinder viscometer. When the instrument is activated, a shear gap is formed between the outer rotor and the inner cylinder, and the slurry in the sample cup is contained within it. The instrument adopts the electronic keys to change the speed, and the traditional mechanical rotation is changed to the single chip microcomputer control, which makes the data more stable in long-term use.

Experimental Data Processing

Rheological Curve

The inner cylinder radius of the viscometer is $R_1 = 1.7245$ cm, the inner cylinder height is $X = 3.8$ cm, and the outer rotor radius is $R_2 = 1.8415$ cm. If the outer rotor rotates at a certain speed ω (r/min), the rotation angle of the torsion spring is represented by the deflection number δ of the pointer on the dial, and the dial has a total number $\psi = 300$ cells. The scale of the torsion spring is $k = 386$ dyn·cm/cell, that is, 386 dyn·cm torque is generated every time one grid is rotated. Based on the above basic instrument parameters, substituting it into Formula $\gamma = \frac{\pi R_2^2 \omega}{15(R_2^2 - R_1^2)}$

gives the relationship between shear rate and rotational speed:

$$\gamma = 1.703\omega \quad (42)$$

According to the measured torque $M = k\psi$, the maximum measured torque of the instrument can be calculated as follows:

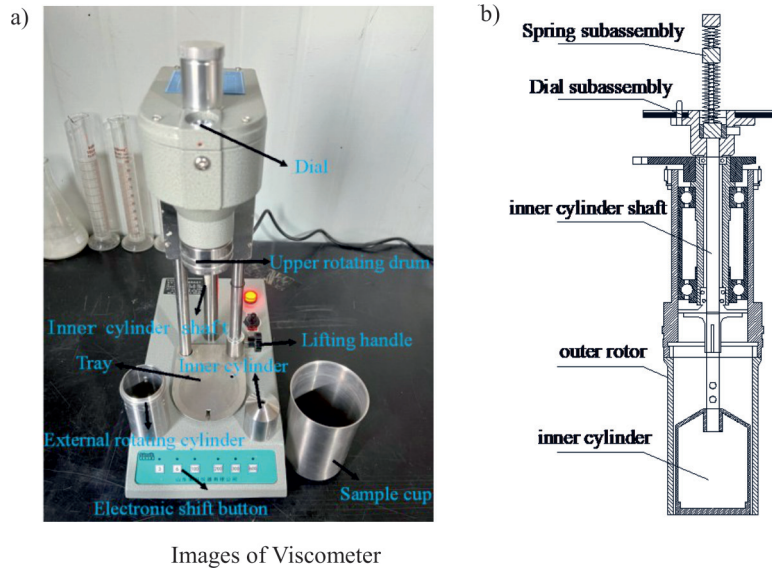
$$M_{\max} = 300 \times 380 = 115800 \text{ dyn} \cdot \text{cm} \quad (43)$$

Substituting equation (43) into shear stress $\tau = \frac{M}{2\pi R_1^2 X}$ gives:

$$\tau_{\max} = 1533 \text{ dyn/cm}^2 \quad (44)$$

Table 2. Content of various components and material characteristics.

SO ₃ /%	MgO/%	Cl ⁻ /%	Initial setting time/min	Final setting time/min	Flexural strength /MPa		Compressive strength /MPa	
					3D	28D	3D	28D
2.4	2.0	0.012	145	200	5.5	7.6	21.6	48.7



Images of Viscometer

Fig. 4. Six speed rotary viscometer of ZNN-D6B type: a) Images of Viscometer, b) Schematic Diagram of Working Principle.

According to Equation (44), the torsion spring coefficient of the instrument can be obtained:

$$E = \frac{\tau_{\max}}{\delta} = \frac{1533}{300} = 5.11 \text{ dyn/cm}^2 / \text{cell} = 0.511 \text{ Pa/cell} \quad (45)$$

Therefore, the relationship between the shear stress and the number of rotating cells is as follows:

$$\tau = 0.511 \delta \quad (46)$$

To sum up, during the experiment, read the number of rotating cells δ corresponding to the torque spring by controlling the rotational speed ω of the viscometer to a certain value. Combining Equations (42) and (46), respectively calculate the shear rate and shear stress corresponding to different rotational speeds, and present the calculated results as a graph to obtain the rheological curve.

Consistency Coefficient Time-Varying Curve

From the above equations can derives the formula for calculating the rheological parameters of power-law slurry:

Rheological index

$$n = 3.3211 \lg \frac{600 \text{ r/min (reading)}}{300 \text{ r/min (reading)}} \quad (47)$$

Consistency coefficient

$$C = \frac{0.511 \times 300 \text{ r/min (reading)}}{511^n} \text{ Pa} \cdot \text{s}^n \quad (48)$$

Therefore, the number of rotating cells at a certain rotational speed can be read in turn at the specified time node, and the corresponding rheological parameters can be calculated by using Equations (47) and (48). The time-varying curve of slurry consistency coefficient can be obtained by plotting the results in the coordinate system.

Experimental Procedure

1. Instrument installation: Rotating the inner cylinder counterclockwise and slowly push it upward to fit with the cone end of the inner cylinder shaft, so as to avoid deformation and damage of the inner cylinder shaft. Then rotate it to the right to install the outer rotor and connect the power.
2. Slurry prepare: Weighing the cement mortar and water required according to the water-cement ratio of slurry designed in the experiment, as shown in Fig. 5. Pouring the weighed materials into the mixing bucket, and use the agitator to mix at high speed to ensure complete mixing, as shown in Fig. 6.
3. Slurry transfer: Pouring the uniformly mixed cement slurry into the sample cup to the black mark inside the cup. Then place the sample cup on the tray,



Fig. 5. Weighing of water and cement.



Fig. 6. Agitator and slurry mixing process.

and slowly lift the tray until the liquid level of the experiment solution in the sample cup is flush with the red scale line above the outer rotor. Stop lifting, tighten the lifting handle, and turn on the switch.

4. Experiment start: 1-Determination of rheological curves: Using the electronic variable speed button to switch the speed step by step from low to high, measure the rotation angle of the torsion spring corresponding to each speed step, and record the data. 2-Determination of consistency coefficient time-varying curves: Start timing, directly adjust the speed to 300 r/min, read the rotation angle of the torsion spring at this time and record. Then quickly change to 600 r/min, read and record the rotation angle of the torsion spring at this time. And repeat the above operations at 5 min, 10 min, 20 min, 30 min and 40 min respectively.
5. Experiment complete: Turn off the power supply, unscrew the lifting handle, lower the tray to the bottom, take down the sample cup, and then turn clockwise to take down the outer rotor and inner cylinder, and clean and dry them.
6. Data processing: The above experimental data shall be processed and calculated according to the data processing method in the chapter "Experimental data processing".

Analysis of Experimental Results

For slurry samples with the same water-cement ratio, they shall be measured at least three times under

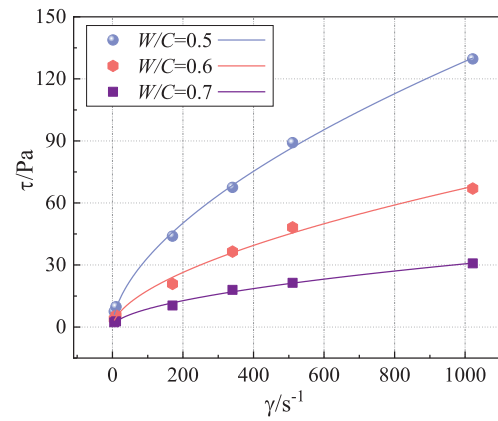


Fig. 7. Rheology curve of Power-law slurry.

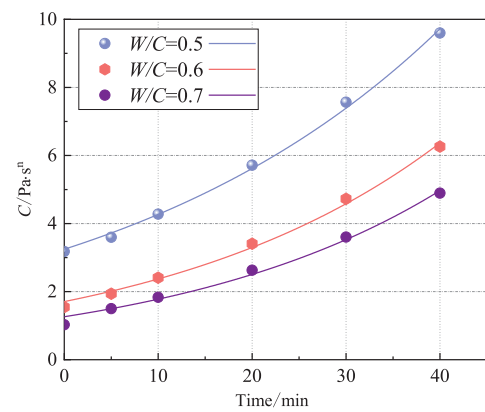


Fig. 8. Consistency coefficient time-varying curve of Power-law slurry.

the same experimental conditions to ensure that their standard deviation is within 5%, and then the average value shall be selected as the final data result. By fitting and analyzing the above results, we can get the rheological curves and consistency coefficient time-varying curves of power-law slurry with different water-cement ratios and their corresponding rheological equation and consistency coefficient time-varying function expression. The results are shown in Fig. 7, Fig. 8 and Table 3.

As shown in Fig. 7 and Fig. 8, the experimental results of power-law slurry have a good fit with the fitted rheological curve and consistency coefficient time varying curve. In Fig. 7, if the shear rate is kept constant, when the water-cement ratio decreases from 0.7 to 0.5, the corresponding shear stress increases with it, and the smaller the water cement ratio, the more obvious the change trend. This is because the viscosity and concentration of the slurry at a small water-cement ratio are larger, which requires a greater shear stress to enable the slurry to shear flow. Secondly, when the water cement ratio is kept constant, the shear rate increases, and the shear stress also increases nonlinearly with it. The rheological curve has obvious power function image change characteristics. In Fig. 8,

Table 3. Constitutive equation and consistency coefficient time-varying equation of Power-law slurry.

Water-cement ratio	Rheological equation (initial)		Time varying equation of consistency coefficient		Time varying law of consistency coefficient		
					Maximum fit value	Minimum fit value	Difference ratio /%
0.5	$\tau=2.2871\gamma^{0.5832}$	$R^2 = 0.99852$	$C(t) = 3.2455e^{0.02743t}$	$R^2 = 0.99697$	9.7228	3.2455	66.62%
0.6	$\tau=1.2218\gamma^{0.58003}$	$R^2 = 0.99185$	$C(t) = 1.7074e^{0.03291t}$	$R^2 = 0.99410$	6.3685	1.7074	73.19%
0.7	$\tau=0.71813\gamma^{0.543}$	$R^2 = 0.99408$	$C(t) = 1.2632e^{0.03424t}$	$R^2 = 0.98992$	4.9691	1.2632	74.58%

the consistency coefficients of the slurry with different water-cement ratios increase with time, and the longer the time, the greater the increase. The change trend of the data presented in the figure conforms to the image characteristics of the exponential function, which is fitted according to the general time-varying function $\mu_p(t) = \mu_0 e^{bt}$ of the slurry consistency coefficient. The fitting results are shown in Table 3.

As shown in Table 3, the rheological equation and consistency coefficient time-varying equation of the power-law slurry with different water-cement ratios are typical power functions and exponential functions, which conform to the variation characteristics of the slurry rheological curves and consistency coefficient time-varying curves, and the fitting results are well correlated with the experimental results, which is consistent with previous research results [29-30]. Secondly, it can be seen that the difference between the maximum consistency coefficient and the minimum consistency coefficient fitted in the process of time change is great, and the greater the water-cement ratio, the greater the difference. In fact, the essence of slurry viscosity change is that the content of flocculated particles in the slurry increases and the particle spacing decreases during the slurry hydration process, which ultimately leads to the increase of slurry viscosity. This change is closely related to the stability of the power-law slurry. The larger the water cement ratio of the slurry, the worse its stability is. Therefore, the greater the variation of the slurry viscosity with time in a certain period of time.

The results of two factors variance analysis of the effect of of hydration time and water-cement ratio on consistency coefficient of power-law slurry were obtained by SPSS, as shown in Table 4. F in the table represents the statistic of F test, which is the ratio of the sum of squares of deviations between groups and within groups to the degree of freedom; P represents the significance coefficient, which is a decreasing indicator of the reliability of the results. F and P are used to evaluate the rationality of the influence of hydration time and water-cement ratio of slurry on rheological parameters of different power-law slurries. The results are usually compared with $F_{\alpha=0.05, \text{crit}}$ and $\alpha = 0.05$ (α is the significance level). R^2 represents the determination coefficient, reflecting the percentage of variance that can be explained by the regression equation in the variance of the dependent variable. If $F > F_{\alpha=0.05, \text{crit}}$ and $P < \alpha = 0.05$, at level $\alpha = 0.05$ hydration time and water-cement ratio of slurry have significant effects on rheological parameters of different power-law slurries, and vice versa [31].

As shown in Table 4, for power-law slurry, $F(W/C) = 52.320 > F_{\alpha=0.05, \text{crit}} = 4.103$, $P(W/C) < 0.05$ and $F(t) = 38.113 > F_{\alpha=0.05, \text{crit}} = 3.326$, $P(t) < 0.05$. The above comparison results show that the water-cement ratio and time of the slurry have significant effects on the consistency coefficient, so it is necessary to consider the combined effects of the two on the consistency coefficient of the slurry. It can be seen from A that the combined effect of water-cement ratio and time on the slurry consistency coefficient is also very significant.

Table 4. Two factors variance analysis of the effect of hydration time and water-cement ratio on consistency coefficient of Power-law slurry.

Slurry flow pattern	Source	Class III sum of squares	DOF	Mean square	F	P	$F_{\alpha=0.05, \text{crit}}$
Power-law slurry (Consistency coefficient C) $R^2 = 0.967$ $R = 0.98$	Water-cement ratio	30.527	2	15.263	52.320	<0.001	4.103
	Time	55.594	5	11.119	38.113	<0.001	3.326
	Error	2.917	10	0.292			
	Total	358.992	18				
	Total after correction	89.038	17				

Results and Discussion

Effectiveness Analysis

In order to verify the effectiveness of the solution of power-law slurry diffusion model in unsaturated media under displacement effect. Degrading Equation (40) to the saturated state produces the following equation:

$$p_{01} = p_w^0 - \frac{\phi R^2 \mu_w \ln R / r_e}{2Kt} + \frac{\left(\frac{\phi R^2}{2t}\right)^n \mu_e (R^{1-n} - r_0^{1-n})}{K_e (1-n)} \tag{49}$$

Yang et al. [32]. studied the power-law slurry and obtained the cylindrical diffusion mechanism formula of time-varying power-law slurry. As follows:

$$p_{02} = p_w^0 + \frac{e^{\beta t}}{1-n} \left(\frac{\mu_e}{K_e}\right) \left(\frac{\phi}{2t}\right)^n (R^{1-n} - r_0^{1-n}) R^{2n} \tag{50}$$

Selecting the calculation parameters: $r_0 = 0.03$ m, $p_w^0 = 2 \times 10^4$ Pa, $\phi = 0.37$, $\mu_w = 1.01 \times 10^{-3}$ Pa·s, $K = 7.5 \times 10^{-10}$ m², $r_e = 1$ m, $t = 20$ s, $S_R = 0.696$. Calculating and comparing Equation (49) with equation (40) and Equation (50) respectively. The results are shown in Fig. 9.

Firstly, comparing Equations (49) and (50), it is found that the forms of two equations are roughly the same. The difference is that compared with Equation (50), Equation (49) further considers the water driven effect of slurry in saturated state. However, the existing research results consider the groundwater as a definite boundary, ignoring the interface condition $v_g = v_w$ and $p_g|_{\varphi=R} = p_{cr} = p_w|_{\varphi=R}$ and boundary condition $p_w|_{\varphi=r_e} = p_w^0$ existing at $\varphi(t) = R$, so that the

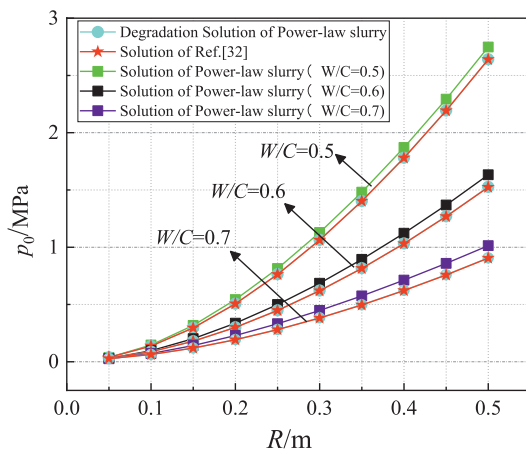


Fig. 9. Comparison of the relationship between slurry diffusion radius and grouting pressure under different.

difference between the two slurry diffusion mechanism equations is characterized in the form of

$$\frac{R^2 \phi \mu_w \ln(r_e / R)}{2Kt}$$

Secondly, it can be seen from Fig. 9 that the difference between the solution degraded to saturated state and the existing solution is extremely small, and compared with the final grouting pressure p_{01} and p_{02} , it can be completely ignored. With the increase of grout diffusion radius R , the larger grouting pressure is required as the driving force to overcome the resistance encountered by the slurry in the stratum and complete the subsequent migration and diffusion, resulting in the increase of grouting pressure p_{01} and p_{02} with the increase of grout diffusion radius R . When the slurry diffusion radius R is constant, with the water cement ratio changing from 0.5 to 0.7, the density and viscosity of the slurry decrease, so the stratum resistance encountered during the slurry diffuses is smaller, so the grouting pressure p_{01} and p_{02} decrease with it. At the same time, under different water-cement ratios, there is an obvious difference between the numerical results of unsaturated and saturated conditions, which will directly affect the grouting effect. The reason is that the degree of saturation and relative permeability are introduced into the solution in unsaturated state, and the stratum is no longer defaulted to be in saturated water-bearing state. According to the following Equations (51) and (52), the value of relative permeability is also related to the degree of saturation of the injected medium. The above parameters exist and have significant effects that cannot be ignored in unsaturated media. The above analysis and verification results fully confirm the validity of the solution presented in this paper and the necessity of considering displacement effect and time-varying of slurry viscosity in unsaturated media.

Numerical Analysis and Discussion

In the numerical example, the soil-water characteristic curve is described by the Van Genuchten model [33]. The above model can be defined as:

$$S_e = \frac{S_r - S_{res}}{S_{sat} - S_{res}} = \left[1 + \left(\frac{p_c}{p_b} \right)^n \right]^{-m} \tag{51}$$

Where S_e is the effective saturation of the liquid phase, S_{res} is the residual saturation, S_{sat} is the saturation in the saturated state, p_b is the intake pressure, p_c is the capillary pressure, i and n are pore distribution parameters, which are related to the pore radii distribution of the soil, $i = 1 - \frac{1}{j}$. In the example,

$p_c = 50$ kPa, $p_b = 35$ kPa, $j = 1.56$, $i = 0.36$, $S_{sat} = 1.00$, $S_{res} = 0$ [34].

According to VG model, the relationship between

relative permeability and degree of saturation of liquid phase is given as follows:

$$k_{rw} = \sqrt{s_e} \left[1 - \left(1 - s_e^{\frac{1}{m}} \right)^m \right]^2 \tag{52}$$

The physical and mechanical parameters of the stratum are as follows: $\mu_w = 1.01 \times 10^{-3} \text{Pa}\cdot\text{s}$, $r_e = 1 \text{ m}$, $p_w^0 = 2 \times 10^4 \text{Pa}$.

Different Water-Cement Ratios

In order to analyze the influence of different water-cement ratios on slurry diffusion radius and grouting pressure. Taking the parameters as follows: grouting pipe radius $r_0 = 0.03 \text{ m}$, soil inherent permeability $K = 7.5 \times 10^{-10} \text{ m}^2$, grouting time $t = 20 \text{ s}$, and soil porosity $\phi = 0.37$, and other parameters remain unchanged. The water-cement ratio is taken successively as 0.5, 0.6 and 0.7. The variation of the relationship between grout diffusion radius and grouting pressure under different slurry water-cement ratios is shown in Fig. 10.

It is seen that when the water-cement ratio W/C is constant, with the increase of slurry diffusion radius, the larger grouting pressure is needed to overcome the resistance encountered by the slurry in the stratum, that is, p_0 increases nonlinearly with R . This change law is applicable to the change relationship between p_0 and R when any other parameter variable remains constant, and vice versa. At the same time, it can be seen that when the slurry diffusion radius is constant, the grouting pressure increases with the decrease of water-cement ratio. This is because W/C has significant influence on the slurry density, plastic viscosity and time-varying coefficient of viscosity. The decrease of W/C will lead to the increase of slurry density and viscosity, which will increase the friction resistance between slurry and solid particles of stratum. Therefore, the larger driving force is required for completing

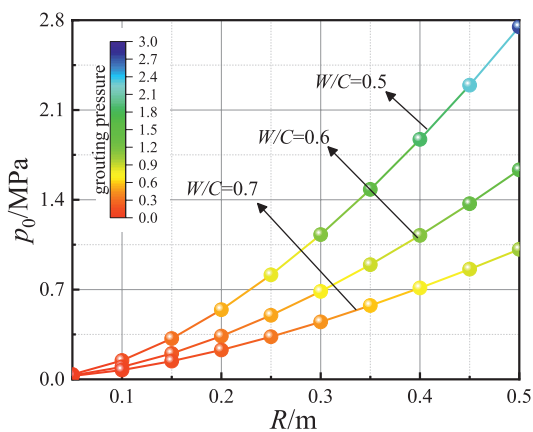


Fig. 10. Influence of water-cement ratio on grouting pressure and slurry diffusion radius.

injection and subsequent migration and diffusion of slurry, resulting in the increase of grouting pressure. Similar studies have shown that the increase of water-cement ratio will lead to the decrease of the strength of the slurry stone body [35]. The above factors should be balanced in order to achieve the best grouting result when preparing cement slurry in engineering practice.

Different Grouting Pipe Radius

In order to analyze the influence of different grouting pipe radius on slurry diffusion radius and grouting pressure. Taking the parameters as follows: $W/C = 0.6$, $K = 7.5 \times 10^{-10} \text{ m}^2$, $t = 20 \text{ s}$, $\phi = 0.37$, and other parameters remain unchanged. The grouting pipe radius is changed gradually from 1.5 cm to 3.5 cm, and the variation of the relationship between slurry diffusion radius and grouting pressure under different grouting pipe radius is shown in Fig. 11.

It is seen that that when the slurry diffusion radius R is constant, the larger the grouting pipe radius r_0 is, the smaller the grouting pressure p_0 required to make the slurry diffuse to a certain range R . It can be seen from Equation (35) that the increase of the grouting pipe radius r_0 directly leads to the increase of the total amount of slurry Q' within a certain grouting time. Therefore, in the same slurry diffusion plane, the grouting pressure required for the slurry to diffuse to a certain range through the grouting pipe of large diameter is less than that of small diameter. Similarly, if the grouting pressure p_0 remains unchanged, the larger the grouting pipe radius r_0 , the larger the slurry diffusion radius R . In fact, the larger the radius of the grouting pipe is, the more difficult it is to place it into the injected medium, and the grouting equipment with higher power is needed to provide power during construction. When analyzing the factors affecting the slurry diffusion range, most of the existing researches focus on factors such as porosity, permeability and water-cement ratio [36]. However, the above analysis results have proved that the grouting pipe radius has a

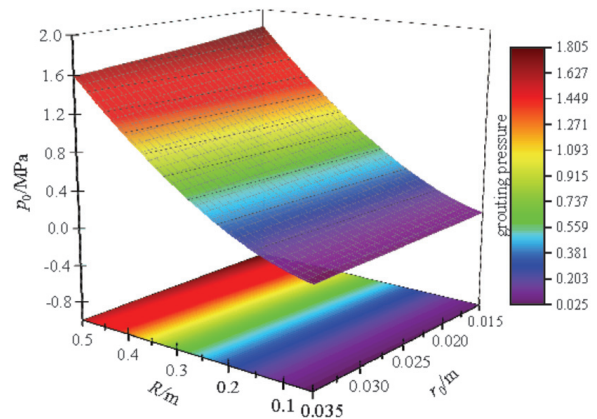


Fig. 11. Influence of grouting pipe radius on grouting pressure and slurry diffusion radius.

significant effect on the slurry diffusion behavior and the prediction of grouting pressure.

Different Soil Inherent Permeabilities

In order to analyze the influence of different soil inherent permeabilities on slurry diffusion radius and grouting pressure. Taking the parameters as follows: $W/C = 0.6$, $r_0 = 0.03$ m, $t = 20$ s, $\phi = 0.37$, and other parameters remain unchanged. The variation of the relationship between slurry diffusion radius and grouting pressure under different soil inherent permeabilities is shown in Fig. 12.

It is seen that the grouting pressure p_0 decreases gradually with the soil inherent permeability K changes from 1.5×10^{-10} m² to 7.5×10^{-10} m² when the slurry diffusion radius R is constant. Because the soil inherent permeability refers to the ability of the injected medium to allow the slurry to pass under a certain pressure difference. It is a macroscopic transport parameter, which can be used to describe the difficulty of driving slurry to diffuse to a certain range. The value of K is firstly related to the porosity of the injected medium, and secondly also inextricably linked to the geometry of the pores in the direction of slurry penetration, the size of the particles and the direction of their arrangement, but not to the various material properties of the slurry. The larger the K value, the better the slurry will pass through the injected medium, the less resistance the slurry will be subjected to per unit volume, and therefore the smaller the grouting pressure will be to drive the slurry to the intended diffusion range.

Different Grouting Times

In order to analyze the influence of different grouting times on slurry diffusion radius and grouting pressure. Taking the parameters as follows: $W/C = 0.6$, $r_0 = 0.03$ m, $K = 7.5 \times 10^{-10}$ m², $\phi = 0.37$, and other parameters remain unchanged. The grouting time is changed successively from $t = 50$ s to $t = 100$ s. The variation of the relationship between slurry

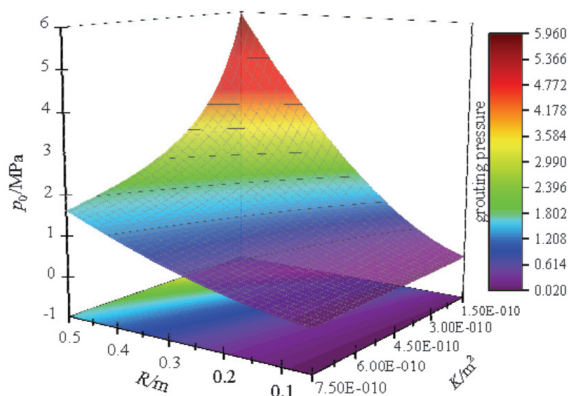


Fig. 12. Influence of soil inherent permeability on grouting pressure and slurry diffusion radius.

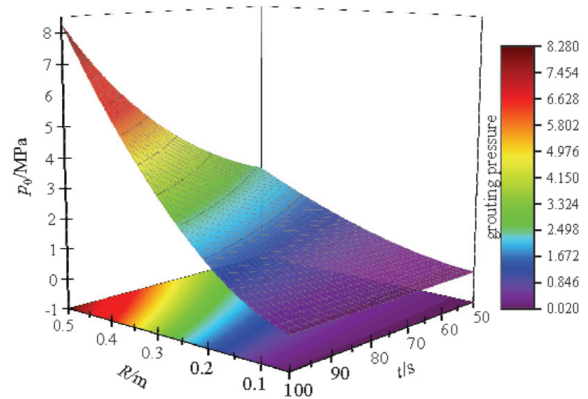


Fig. 13. Influence of grouting time on grouting pressure and slurry diffusion radius.

diffusion radius and grouting pressure under different grouting times is shown in Fig. 13.

The viscosity of slurry will change with the passage of time due to the hydration of slurry. It is seen that the grouting pressure p_0 increases nonlinearly with the increase of grouting time t when the slurry diffusion radius is constant, and with the increase of slurry diffusion radius R , its change amplitude is larger. This is because with the increase of grouting time t , the content of flocculated particles in the slurry increases, and the particle spacing decreases, so that the viscosity of the power-law slurry increases. Thus, the friction effect between slurry and solid particles skeleton is enhanced after entering the injected medium, and the resistance encountered by the slurry keeps growing as it diffuses. In addition, the viscosity and density of power-law slurry are larger, which will produce inhomogeneous retention and deposition in the migration and diffusion process over time. Then the slurry diffusion channel is blocked, so that the grouting pressure p_0 increases with the increase of grouting time t . The time-varying effect of slurry viscosity becomes more and more significant when the slurry diffusion radius continues to expand. In the process of infiltration and diffusion of slurry, its rheological parameters show obvious dependence on the grouting time [37-38]. Therefore, whether the grouting time is considered or not directly affects the grouting effect.

Different Soil Porosities

In order to analyze the influence of different soil porosities on slurry diffusion radius and grouting pressure. Taking the parameters as follows: $W/C = 0.6$, $r_0 = 0.03$ m, $K = 7.5 \times 10^{-10}$ m², $t = 20$ s, and other parameters remain unchanged. The soil porosity is changed successively from $\phi = 0.37$ to $\phi = 0.47$. The variation of the relationship between slurry diffusion radius and grouting pressure under different soil porosities is shown in Fig. 14.

It is seen that the grouting pressure p_0 is positively correlated with the soil porosity ϕ when the slurry

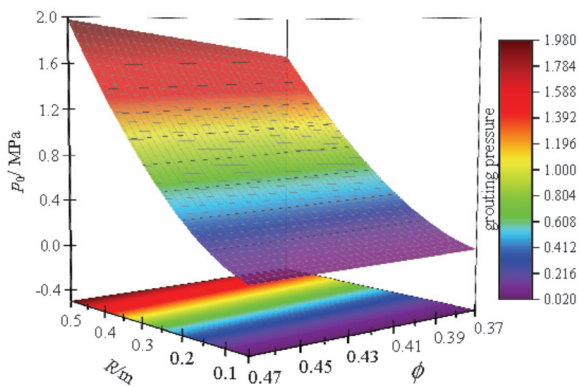


Fig. 14. Influence of soil porosity on grouting pressure and slurry diffusion radius.

diffusion radius is constant, and the variation trend becomes more obvious with the increase of the slurry diffusion radius. The soil porosity directly reflects the compactness of the injected medium, and it is an important parameter that directly affects the infiltration and diffusion behavior of the slurry in the porous medium. The increase of porosity means that the volume of pores in the injected medium increases, so the contact area between the slurry and the stratum particles increases, resulting the resistance encountered by the slurry increases accordingly. And the larger the porosity, the stronger the retardation effect of pore fluid on slurry. At the same time, the temporal and spatial variation of porosity is often accompanied by the occurrence of infiltration and filtration [18], which decreases the soil permeability and increases the difficulty of slurry injection. In order to eliminate the influence of the above factors, a larger grouting pressure is needed as the driving force.

Conclusions

1. Combined with the rheological equation and the viscosity time-varying function of power-law slurry, the rheological equation of time varying power-law slurry is obtained. Analyzing the laminar motion of power-law slurry in a circular tube with radius H , and obtain the seepage movement equation of time-varying power-law slurry.
2. The slurry cylindrical diffusion model and displacement model are established. Based on the above models and basic equations, combined with the corresponding boundary conditions and interface conditions, the analytical expression describes the relationship between grouting parameters, physical and mechanical parameters and grouting pressure is obtained.
3. The rheological curves and equations of power-law slurry with different water-cement ratios are obtained by rheological experiment. And the time-varying curves and time-varying equations of

consistency coefficient of power-law slurry with different water-cement ratios are obtained by time-varying characteristic experiment of rheological parameters. It can be seen that no matter how large the water-cement ratio is, its consistency coefficients all show positively correlated exponential change with increasing time.

4. The influence laws of many factors affecting the slurry diffusion behavior are analyzed and discussed through numerical examples. The results show that: When the parameters such as water-cement ratio, grouting time, grouting pipe radius, soil inherent permeability and porosity are respectively controlled to be constant, the grouting pressure increases nonlinearly with the increase of grout diffusion radius, indicating that the farther the slurry diffusion range is, the stronger the effect of stratum resistance is. When the slurry diffusion radius is constant, the water-cement ratio, the grouting pipe radius and the soil inherent permeability are negatively correlated with the change of grouting pressure, while the grouting time and the soil porosity are positively correlated with the change of grouting pressure.

Acknowledgments

This work was supported by the National Natural Science Foundation of China (Nos. 11962016 and 51978320), the Foundation for Innovation Groups of Basic Research in Gansu Province (No. 20JR5RA478), and the Lanzhou University of Technology Hongliu Outstanding Youth Talent Support Program Project. The authors are grateful to the reviewers for their insightful and constructive comments.

Conflict of Interest

The authors declare no conflict of interest.

Data Availability Statement

The datasets generated during and/or analysed during the current study are available from the corresponding author on reasonable request.

References

1. LI M.T., ZHANG X., KUANG W., ZHOU Z. Grouting reinforcement of shallow and small clearance tunnel. *Pol. J. Environ. Stud.* **30** (3), 2609, **2021**.
2. OEZCELIK M. Foundation consolidation grouting applications in Deriner Dam and Hydroelectric Power Plant (Artvin, Turkey). *B. Eng. Geol. Environ.* **73** (2), 493, **2014**.
3. CARRANZA-TORRES C. Analytical and numerical study of the mechanics of rockbolt reinforcement around tunnels in rock masses. *Rock Mech. Rock Eng.* **42** (2), 175, **2009**.

4. RUAN W. Research on diffusion of grouting and basic properties of grouts. *Chin. J. Geotech. Eng.* **27** (1), 69, **2005**.
5. ZHAO Z.K., WANG T.H., JIN X. Study on permeation grouting rules for loess and method for predicting migration radius. *KSCE J. Civ. Eng.* **25** (8), 2876, **2021**.
6. FU Y.B., WANG X.L., ZHANG S.Z., YANG Y. Modelling of permeation grouting considering grout self-gravity effect: Theoretical and Experimental Study. *Adv. Mater. Sci. Eng.* **2019**, 16, **2019**.
7. REN B., MU W.Q., XIAO D.C. Grouting mechanism in water-bearing fractured rock based on two-phase flow. *Geofluids.* **2021**, 18, **2021**.
8. ZOU L.C., HAKANSSON U., CVETKOVIC V. Analysis of Bingham fluid radial flow in smooth fractures. *J. Rock Mech. Geotech.* **12** (5), 1112, **2020**.
9. FUNEHAG J., THORN J. Radial penetration of cementitious grout-Laboratory verification of grout spread in a fracture model. *Tunn. Undergr. Sp. Tech.* **72**, 228, **2018**.
10. FUNEHAG J., CLAESSEON J. How the pressure build-up affects the penetration length of grout-new formulation of radial flow of grout incorporating variable pressure. *Grouting*, **288**, 143, **2017**.
11. MU W.Q., LI L.C., LIU X.G., ZHANG L.Y., ZHANG Z.L., HUANG B., CHEN Y. Diffusion-hydraulic properties of grouting geological rough fractures with power-law slurry. *Geomech. Eng.* **21** (4), 357, **2020**.
12. ZOU L.C., HAKANSSON U., CVETKOVIC V. Yield-power-law fluid propagation in water-saturated fracture networks with application to rock grouting. *Tunn. Undergr. Sp. Tech.* **95**, 12, **2020**.
13. ZOU L.C., HAKANSSON U., CVETKOVIC V. Radial propagation of yield-power-law grouts into water-saturated homogeneous fractures. *Int. J. Rock Mech. Min.* **130**, 12, **2020**.
14. ZHANG W. The grouting diffusion model of power-law fluid in single fracture. *Appl. Mech. Mater.* **477-478**, 524, **2014**.
15. RAHMAN M., HAKANSSON U., WIKLUND J. In-line rheological measurements of cement grouts: Effects of water-cement ratio and hydration. *Tunn. Undergr. Sp. Tech.* **45**, 34, **2015**.
16. ZHU D.X., GUO Y., WANG W., GUO G.Y., AN T.L. Grouting reinforcement technique in wind oxidation zone by power law superfine cement slurry considering the time-varying rheological parameters. *Adv. Civ. Eng.* **2019**, 10, **2019**.
17. GUO T.T., ZHANG Z.W., YANG Z.Q., ZHU Y.Y., YANG Y., GUO Y.H., WANG R.C., ZHANG B.H., FANG Y.C., YU D.L., MI Y.P., SU J.K., LIU H., ZHANG J., GUO Y.F., WANG H.L. Penetration grouting mechanism of time-dependent power-law fluid for reinforcing loose gravel soil. *Minerals-Basel.* **11** (12), 17, **2021**.
18. ZHANG Q.Q., LI H.T., CUI W., ZHAO Y.H., WANG S.L., XU F. Analysis of grout diffusion of postgrouting pile considering the time-dependent behavior of grout viscosity. *Int. J. Geomech.* **21** (11), 10, **2021**.
19. ZOU L.C., HAKANSSON U., CVETKOVIC V. Two-phase cement grout propagation in homogeneous water-saturated rock fractures. *Int. J. Rock Mech. Min.* **106**, 243, **2018**.
20. YE F., QIN N., HAN X., LIANG X., GAO X., YING K.C. Displacement infiltration diffusion model of power-law grout as backfill grouting of a shield tunnel. *Eur. J. Environ. Civ. En.* **26** (5), 1820, **2022**.
21. YANG Q., GENG P., TANG R., ZHAO B.B., GUO X.Y., HE Y. Slurry seepage and diffusion mechanism of shield tunnel backfilling grouting in unsaturated stratum. *Chin. Railw. Sci.* **41** (6), 100, **2020**.
22. WANG Q., WANG S.Y., SU W., PAN D.Y., ZHANG Z., YE W.M. Interpretation of grouting characteristics in unsaturated sand from the perspective of water-air interface. *Acta Geotech.* **17** (7), 2943, **2022**.
23. LIU X.L., WANG F., HUANG J., WANG S.J., ZHANG Z.Z., NAWNIT K. Grout diffusion in silty fine sand stratum with high groundwater level for tunnel construction. *Tunn. Undergr. Sp. Tech.* **93**, 11, **2019**.
24. KONG X.Y. Advanced seepage mechanics. University of Science and Technology of China Press: Beijing, China, **2020**.
25. AL-ZAIDI E., NASH J., FAN X.F. Effect of CO₂ phase on its water displacements in a sandstone core sample. *Int. J. Greenh. Gas. Con.* **71**, 227, **2018**.
26. AL-ZAIDI E., EDLMANN K., FAN X.F. Gaseous CO₂ behaviour during water displacement in a sandstone core sample. *Int. J. Greenh. Gas. Con.* **80**, 32, **2019**.
27. TRAN T.Q.M.D., NEOGI P., BAI B. Stability of CO₂ displacement of an immiscible heavy oil in a reservoir. *SPE J.* **22**(2), 539, **2017**.
28. French petroleum and natural gas exploration and development union. Manual of Rheology of Drilling Mud and Cement Slurry. Petroleum Industry Press: Beijing, China, **1984**.
29. DU J., ZHU W.W., FENG G.J., LIANG W., SHEN X.G., XU C.F. Rheological characteristics of power-law cement grouts based on time-dependent behavior of viscosity. *Chem. Eng. Trans.* **51**, 1111, **2016**.
30. YANG Z.Q., HOU K.P., GUO T.T. Research on time-varying behavior of cement grouts of different water-cement ratios. *Appl. Mech. Mater.* **71-78**, 4398, **2011**.
31. YANG Z.Q., DING Y., MI Y.P., ZHU Y.Y., YANG Y., GUO Y.H., ZHANG B.H., LI S.H., SU J.K., CHEN J.Z., XU W.Z., LIU W.L., LIU H., WANG Y.D. Comprehensive effect of the time and water-cement ratio on the rheological properties of power-law cement grouts. *Geofluids.* **2021**, 12, **2021**.
32. YANG Z.Q., NIU X.D., HOU K.P., ZHOU Z.H., LIANG W., GUO Y.H., LU Y.F., YANG B.J., CHENG Y. Columnar diffusion of cement grout with time dependent rheological parameters. *Chin. J. Rock Mech. Eng.* **34** (7), 1415, **2015**.
33. M. T.H. VAN G. A closed-form equation for predicting the hydraulic conductivity of unsaturated soils. *Soil Sci. Soc. Am. J.* **44** (5), 892, **1980**.
34. HU R., CHEN Y.F., ZHOU C.B. Solid-liquid-gas three-phase coupling analysis of soil slope during rainfall infiltration process. *Chin. Sci. Technol. Sci.* **41** (11), 1469, **2011**.
35. YE F., QIN N., LIANG X., HAN X.B., HAN X. Microscopic model analysis of shield tunnel backfill grouting based on displacement effect. *J. Southwest Jiaotong U.* **57** (2), 339, **2022**.
36. JIANG D.H., CHENG X.Z., LUAN H.J., WANG T.X., ZHANG M.G., HAO R.Y. Experimental investigation on the law of grout diffusion in fractured porous rock mass and its application. *Processes.* **6** (10), 16, **2018**.
37. ZHU Z.J., WANG M., LIU R.T., ZHANG H.S., ZHANG C.Y., LIU Y.K., BAI J.W., ZHANG L.Z. Study of the viscosity-temperature characteristics of cement-sodium silicate grout considering the time-varying behaviour of viscosity. *Constr. Build. Mater.* **306**, 11, **2021**.
38. ZHANG J.F., WANG F.Y., ZHANG H.M. Mechanism of fracture grouting considering the time dependency of viscosity. *Arabian J. Geosci.* **15** (2), 14, **2022**.